Model for hydrothermal growth of rutile wires and the associated development of defect structures

Andreas Wisnet,[†] Sophia Betzler,[†] Rachel V. Zucker,[‡] James Dorman,[¶] Peter Wagatha,[†] Sonja Matich,[§] Eiji Okunishi,[‖] Lukas Schmidt-Mende,[¶] and Christina Scheu[*,†,⊥]

Department of Chemistry & Center for Nanoscience, Ludwig-Maximilians-University, Munich, Germany, Department of Materials Science and Engineering, Massachusetts Institute of Technology, Cambridge MA, USA, Department of Physics, University of Konstanz, Konstanz, Germany, Walter Schottky Institut, Technical University, Garching, Germany, JEOL Ltd., Tokyo, Japan, and Max-Planck-Institut für Eisenforschung GmbH, Düsseldorf, Germany

E-mail: scheu@mpie.de

[*]To whom correspondence should be addressed
[†]Department of Chemistry & Center for Nanoscience, Ludwig-Maximilians-University, Munich, Germany
[‡]Department of Materials Science and Engineering, Massachusetts Institute of Technology, Cambridge MA, USA
[¶]Department of Physics, University of Konstanz, Konstanz, Germany
[§]Walter Schottky Institut, Technical University, Garching, Germany
[‖]JEOL Ltd., Tokyo, Japan
[⊥]Max-Planck-Institut für Eisenforschung GmbH, Düsseldorf, Germany

Supporting Information

Table 1: Hydrothermal synthesis conditions of the samples

Sample name	Temperature	Duration	$Ti(OBu)_4$	NaCl
A	150 $°C$	3 h	58 $mmol/L$	0.25 mol/L
B	150 $°C$	20 h	58 $mmol/L$	0.00 mol/L
C	150 $°C$	3 h	58 $mmol/L$	0.06 mol/L
$V_{H_2O} = V_{HCl} = 5\ mL$				

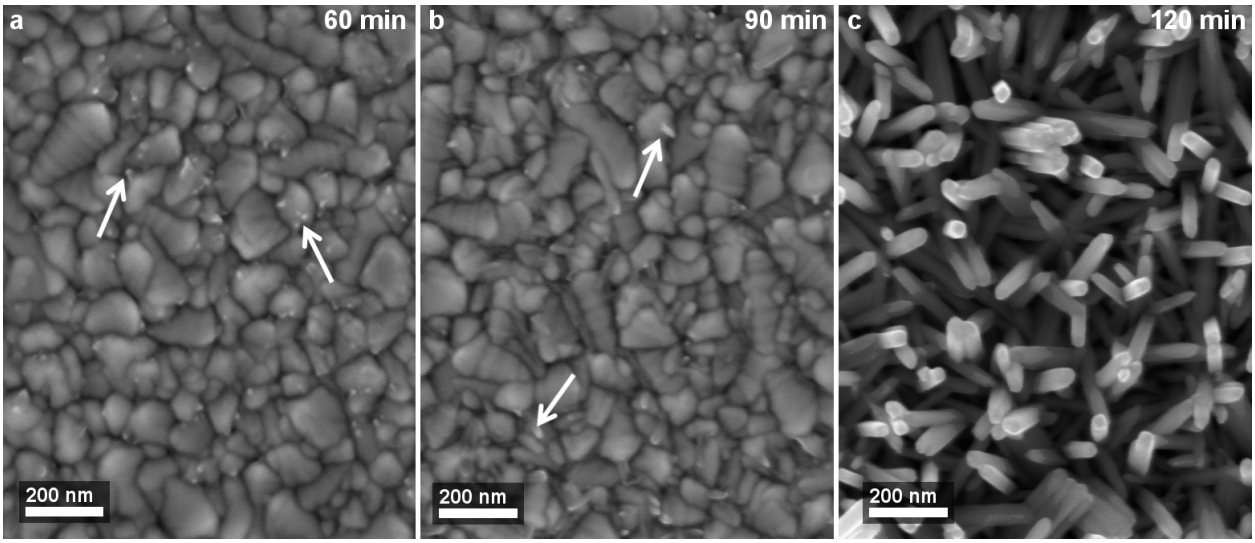

SI Figure 1: SEM images of the crystals at the start of the nanowire growth. a) After 60 minutes at 150 $°C$, the first crystallites can be seen on the FTO substrate. b) During the following 30 minutes, small nanowires start to develop. c) After 120 minutes, the FTO is covered by standing nanowires with an average width of 32 nm.

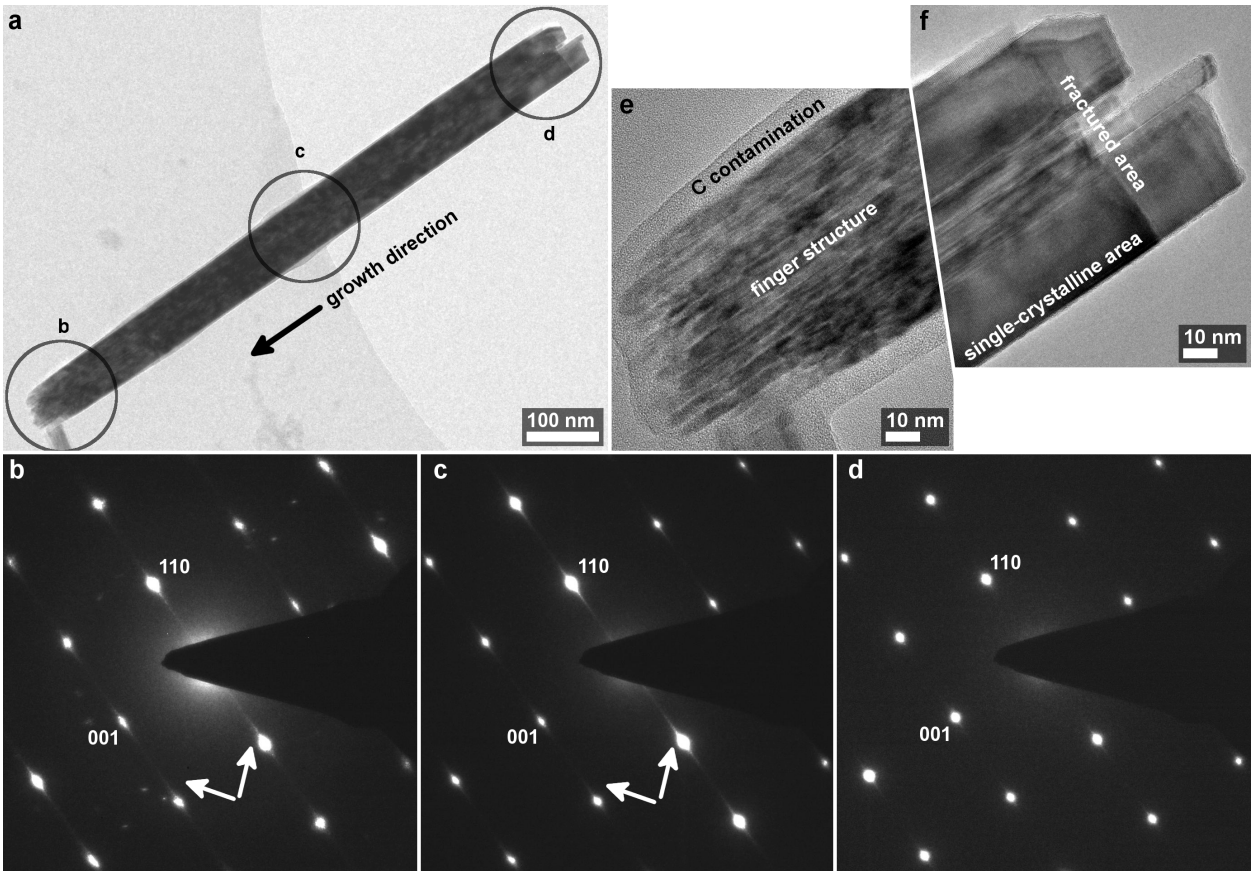

SI Figure 2: Single nanowire and corresponding diffraction patterns (left to right): a) BF image of a typical rutile nanowire. b-d) ED patterns as marked in a). The streaks caused by the finger structures are indicated by arrows in b) (top of the wire) and c) (middle of the wire), and are largely diminished in d) (near bottom of the wire). e) and f) show higher magnifications of e) the wire tip, prominently including the finger structure and f) the wire bottom at its fractured area, showing a wide single-crystalline area surrounding the first fingers in the center of the wire.

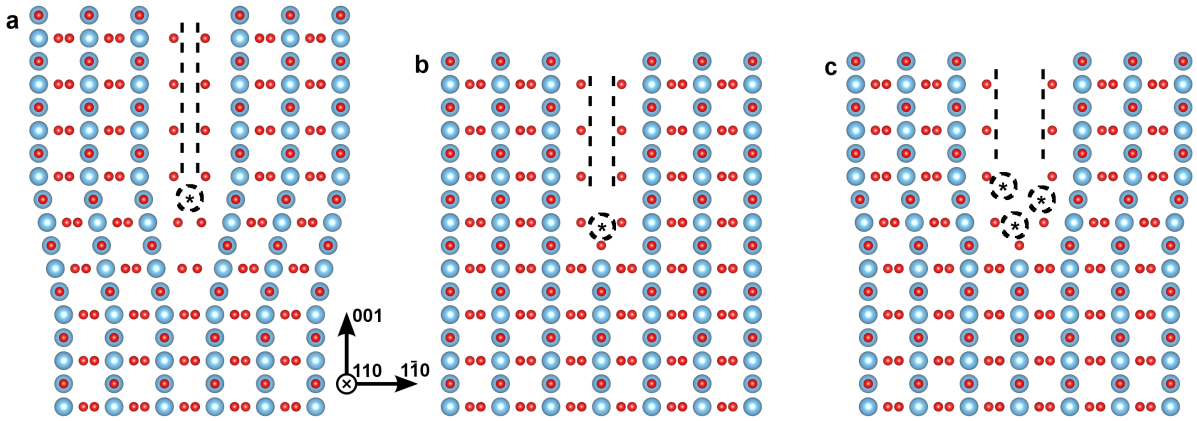

SI Figure 3: a), b) and c) show possible projected atomic configurations at the origin of the finger structure. Blue spheres represent Ti ions, red spheres represent O ions. The black dashed lines indicate the free internal surfaces. An asterisk indicates possible positions of growth-constricting ions. *N.B.*, these schematics are presented only to benefit the readers' understanding of the proposed defect structure. The respective atomic configuration might be far more disarranged than proposed here, specifically at the free internal surfaces. For a more accurate understanding of the atomic configuration, DFT calculations would be needed. Additionally, one could imagine a variety of modifications at the free internal surfaces, including oxygen vacancies, double-bonded oxygen, residues like OH^- groups and Cl^-, etc.

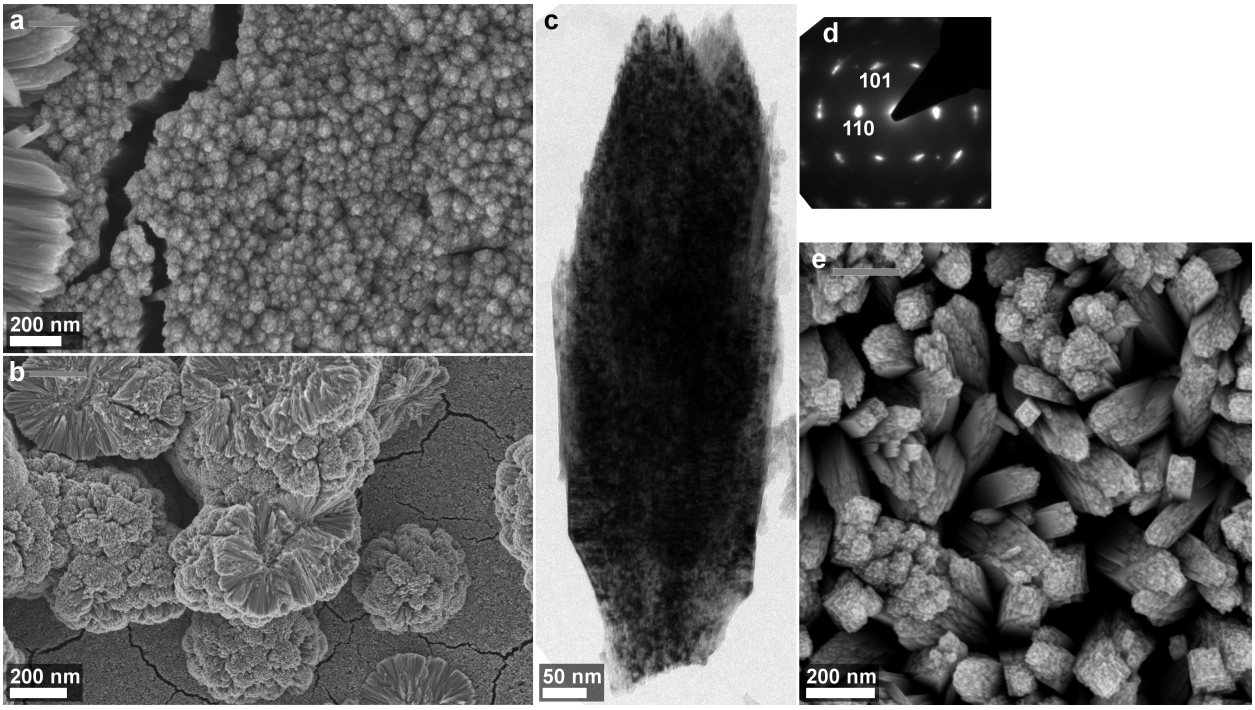

SI Figure 4: Morphology of the nanostructures obtained from an HNO_3-based synthesis. a,b) SEM top view shows a compact layer and larger, flower-like spherical structures. c) TEM BF image of a wire stemming from the sample shown in a). The diameter of the nodule seems to be defined by the packing of the wires. A speckled contrast hints towards a multitude of defects. d) The ED pattern from the nodule in c) shows that the optical axis is $[1\bar{1}\bar{1}]$ and the crystal phase is rutile. e) SEM top view of the structures obtained from the HNO_3-based synthesis with 0.3 mol/L NaCl. The single rutile nanowires are distinguishable.